



Computed Tomography of the Spine

Systematic Review on Acquisition and Reconstruction Techniques to Reduce Radiation Dose

Michael Dieckmeyer¹ · Nico Sollmann^{1,2,3} · Karina Kupfer¹ · Maximilian T. Löffler^{1,4} · Karolin J. Paprottka¹ · Jan S. Kirschke^{1,2} · Thomas Baum¹

Received: 10 June 2022 / Accepted: 10 October 2022 / Published online: 22 November 2022
© The Author(s) 2022

Abstract

The introduction of the first whole-body CT scanner in 1974 marked the beginning of cross-sectional spine imaging. In the last decades, the technological advancement, increasing availability and clinical success of CT led to a rapidly growing number of CT examinations, also of the spine. After initially being primarily used for trauma evaluation, new indications continued to emerge, such as assessment of vertebral fractures or degenerative spine disease, preoperative and postoperative evaluation, or CT-guided interventions at the spine; however, improvements in patient management and clinical outcomes come along with higher radiation exposure, which increases the risk for secondary malignancies. Therefore, technical developments in CT acquisition and reconstruction must always include efforts to reduce the radiation dose. But how exactly can the dose be reduced? What amount of dose reduction can be achieved without compromising the clinical value of spinal CT examinations and what can be expected from the rising stars in CT technology: artificial intelligence and photon counting CT? In this article, we try to answer these questions by systematically reviewing dose reduction techniques with respect to the major clinical indications of spinal CT. Furthermore, we take a concise look on the dose reduction potential of future developments in CT hardware and software.

Keywords Multi-detector computed tomography · Dose reduction · Low dose · Image reconstruction · Image acquisition

Abbreviations

AEC	Automatic exposure control
AI	Artificial intelligence
AIDR	Adaptive iterative dose reduction
AIS	Adolescent idiopathic scoliosis
ASIR	Adaptive statistical iterative reconstruction

AUC	Area under the ROC curve
BC	Cervical spine and brain scan
BMD	Bone mineral density
BMI	Body mass index
CAP	Chest, abdomen and pelvis scan
CNN	Convolutional neural network

✉ Michael Dieckmeyer
michael.dieckmeyer@tum.de

Nico Sollmann
nico.sollmann@tum.de

Karina Kupfer
karina.kupfer@tum.de

Maximilian T. Löffler
m.loeffler@tum.de

Karolin J. Paprottka
karolin.paprottka@tum.de

Jan S. Kirschke
jan.kirschke@tum.de

Thomas Baum
thomas.baum@tum.de

- ¹ Department of Diagnostic and Interventional Neuroradiology, School of Medicine, Klinikum rechts der Isar, Technical University of Munich, Munich, Germany
- ² TUM-Neuroimaging Center, Klinikum rechts der Isar, Technical University of Munich, Munich, Germany
- ³ Department of Diagnostic and Interventional Radiology, University Hospital Ulm, Ulm, Germany
- ⁴ Department of Diagnostic and Interventional Radiology, University Medical Center Freiburg, Freiburg im Breisgau, Germany

CNR	Contrast-to-noise ratio
CT	Computed tomography
CTDI _{vol}	Volumetric CT dose index
DA	Dual acquisition
DECT	Dual energy CT
DLP	Dose length product
E	Effective dose
FBP	Filtered back projection
FEA	Finite element analysis
HIR	Hybrid iterative reconstruction
HU	Hounsfield units
ICC	Intraclass correlation coefficient
IMR	Iterative model reconstruction
IOA	Interobserver agreement
IQ	Image quality
IR	Iterative reconstruction
IVD	Intervertebral disc
IVF	Intervertebral foramen
KV	Tube voltage
LBP	Low back pain
LD	Low dose
LD-CT	Low dose CT
LDD	Lumbar disc disease
LP	Lumbar puncture
MA	Tube current
MA _s	Tube current-time product
MBIR	Model-based iterative reconstruction
MDCT	Multi-detector CT
MRI	Magnetic resonance imaging
MSCT	Multi-slice CT
NA	Not available
PCCT	Photon counting CT
PRI	Periradicular infiltration
PRISMA	Preferred reporting items for systematic reviews and meta-analyses
ROC	Receiver operating characteristics
ROI	Region of interest
SA	Single acquisition
SAFIRE	Sinogram-affirmed iterative reconstruction
SD	Standard dose
SD-CT	Standard dose CT
SIR	Statistical iterative reconstruction
SMA	Spinal muscular atrophy
SNR	Signal-to-noise ratio
SSCT	Single-slice CT
STD	Standard position
SWIM	Swimmer's position
ULD	Ultralow dose
ULD-CT	Ultralow dose CT
VF	Vertebral fracture

Key Points

- Spinal CT has high potential for dose reduction of 50% or more for the majority of clinical applications.
- Options and limitations of dose reduction are highly dependent on the clinical indications and application-specific techniques can further increase the achievable dose reduction.
- Additional dose reduction can be expected from the clinical transition of artificial intelligence and photon counting CT in the upcoming years.

Introduction

The number of computed tomography (CT) examinations performed has been on the rise for decades [1–3]. Increases in clinical application are related to technical developments, wider availability, and physician and patient demands [1, 2]. CT is at the forefront of imaging for multiple purposes, spanning from regular oncologic staging to acute imaging in the emergency trauma setting, contributing significantly to accurate diagnosis, optimized patient management, and improved treatment; however, the use of CT is inherently accompanied by exposure to ionizing radiation, which may cause radiation-induced malignancies [4, 5]. More specifically, it is assumed that about 2% of future cancer cases will be attributable to current application of imaging techniques [3, 6]. Thus, a general principle is to keep radiation exposure as low as reasonably achievable (ALARA principle) [7, 8]; however, in daily clinical routine, CT-related radiation exposure still varies considerably within and across institutions, given that well-defined and ubiquitous reference standards are frequently missing [9, 10]. One relevant aspect is that general recommendations are hard to determine considering the various scanner models and technologies, which may exert an impact on radiation exposure during scanning of different body regions.

CT examinations of the spine are performed for different indications including fracture detection and trauma evaluation, assessment of degenerative changes, postoperative complications, and guidance of interventional procedures, such as periradicular infiltration (PRI) [11–13]. Particularly in musculoskeletal and neuroradiology departments, spinal CT constitutes a large proportion of the daily workload. Evidently, the most effective way to reduce CT-related radiation exposure is to use the technique only when the clinical value outweighs the risks and costs. Aside from that, various developments have emerged on both the acquisition and the reconstruction sides to achieve an optimized trade-off between image quality (IQ) and radiation exposure [14, 15]. Among others, dose reduction techniques include shielding of radiosensitive organs [16], beam-shaping filters [17] and, most importantly, the optimization of acquisition param-

ters, including tube voltage (kV), tube current, voxel size and slice thickness. Tube current is expressed either directly (as mA) or indirectly in terms of tube current-time product (as mAs). Different parameter combinations can lead to entirely different IQ at the same radiation dose.

In clinical CT examinations, radiation exposure is normally controlled via tube current modulation, which nowadays is usually achieved by means of automatic exposure control (AEC) [18, 19]. By adjusting the tube current to the patient's habitus in the axial plane and along the z-axis, a considerable dose reduction can be achieved. Tube current reduction results in a decreased patient dose, as the amount of generated X-ray photons is directly proportional to the tube current [20]; however, image noise increases exponentially, mostly driven by Poisson noise. Exponential noise increase can be avoided by pulse-width modulation of tube current or X-ray flux. This technique, termed sparse-sampling CT, reduces projections generated during a 360° gantry rotation while the dose for each individual projection remains constant. Technical implementations are challenging as they require high voltage fast switching electrical elements or fast shuttering of the X-ray source [21–23].

Any dose reduction technique usually comes at the cost of increased image noise and artifacts. Adequate image reconstruction techniques can mitigate these drawbacks and are therefore a major component of CT dose reduction.

Filtered back projection (FBP) is an analytical reconstruction algorithm relying on the exact mathematical relation between measured projection and reconstructed image data. The speed and robustness of FBP have made it the workhorse of CT reconstruction for decades [15, 24]; however, the assumption of noise-free data and the amplification of noise by the filter severely limit the quality of FBP-reconstructed CT images. In contrast, iterative reconstruction (IR) techniques can reduce image noise through iterative filtering or close to reality physical modeling of the data acquisition process [15]. IR algorithms can be categorized into three stages. Image domain-based reconstruction was the first clinically approved technique in 2009 and features high reconstruction speed; however, noise reduction is limited due to the rather simple iterative denoising only in image space. Hybrid IR algorithms, such as iDose (Philips Healthcare, Best, The Netherlands), ASIR (GE Healthcare, Milwaukee, WI, USA), or SAFIRE (Siemens Healthineers, Erlangen, Germany), feature increased noise reduction and reconstruction time through iterative filtering of both projection and image data. The last stage is represented by model-based IR algorithms (MBIR), which use advanced models in an iterative process of backward and forward projections. They achieve the highest level of noise reduction and ensuing dose reduction but are also computationally most demanding.

The emergence of artificial intelligence (AI) bears great potential for further dose reduction at almost all stages of CT imaging. On the acquisition side, AI-based algorithms have been developed to automatically position the patient at the isocenter using an infrared camera, select the scan range for the required anatomical coverage, or determine tube parameters, in order to optimize patient exposure [25]. On the reconstruction side, AI can be applied to denoise reconstructed images or even perform the reconstruction itself [15, 25]. One common approach is to train a convolutional neural network (CNN) with (simulated) low dose (LD) or artificially noise-enhanced data to reconstruct standard dose (SD) high-quality CT images [26–29]. The application of a CNN is computationally inexpensive once it is trained and validated, when compared to MBIR algorithms. Besides improved IQ, noise reduction, and artifact reduction, reconstruction speed is thus another benefit of AI-based reconstruction. The use of AI in CT imaging will further reduce the required dose; however, study results usually cannot be readily generalized as AI networks are trained on specific datasets. This lack of generalizability must first be addressed to translate AI-based dose reduction to the patient and the ultimate clinical set-up.

Dose reduction techniques are increasingly being used for spinal CT; however, they have not been systematically reviewed yet. Therefore, we aimed to systematically review dose reduction and clinical applications of LD-CT on the spine. Our objective was to determine the degree of clinically achievable dose reduction and the effects on IQ, diagnostic confidence, and patient outcomes. For this purpose, we focused on four major clinical indications: (i) vertebral fractures (VF) and spinal trauma, (ii) spinal degeneration, (iii) perioperative evaluation and (iv) interventional procedures.

Material and Methods

Search Strategy

A search of the online database PubMed (<http://www.ncbi.nlm.nih.gov/pubmed>) was performed to identify studies evaluating methods to reduce radiation dose for spinal CT with respect to the following four clinical indications: (i) VF and spinal trauma, (ii) spinal degeneration, (iii) perioperative evaluation, and (iv) interventional procedures. Studies on CT dose reduction for evaluation of spinal metastases and inflammation were very scarce and therefore not included. The search was conducted by two persons (radiologists with 7 and 4 years of experience, respectively) without a beginning search date (search end date: 12 April 2022). Uncertainties about inclusion of a respective article, if present, were resolved by consensus

through discussion with a third reviewer (board-certified consultant in radiology, 11 years of experience).

The literature search was performed according to the preferred reporting items for systematic reviews and meta-analyses (PRISMA) guidelines [30, 31]. The used search terms for PubMed are available in the appendix.

Inclusion Criteria

Studies were included if they met the following inclusion criteria: (1) study population: human studies including adult or pediatric patients; (2) study design: retrospective or prospective; (3) indications: diagnostic CT for present or suspected spinal pathology, CT for spinal intervention planning or guidance, or perioperative spinal CT; (4) scanning type: noncontrast and/or contrast-enhanced CT covering the entire spine or parts of the spine; (5) purpose: comparison of LD to SD protocols through CT data acquired at different dose levels, CT data acquired at a single dose level and additionally simulated at different dose levels, or CT data including a dose comparison between patient subgroups.

Exclusion Criteria

Studies were not considered if they met the following exclusion criteria: (1) article type: case reports, case series, conference abstracts, letters, editorials, reviews, meta-analyses, or surveys; (2) language of publication other than English;

(3) studies in cadavers, phantoms, or animals; (4) different acquisition technique (e.g., cone beam CT, fluoroscopy, conventional radiography); (5) studies with other purposes (e.g., comparison of shielding techniques, medical staff radiation exposure report).

Extraction of Data

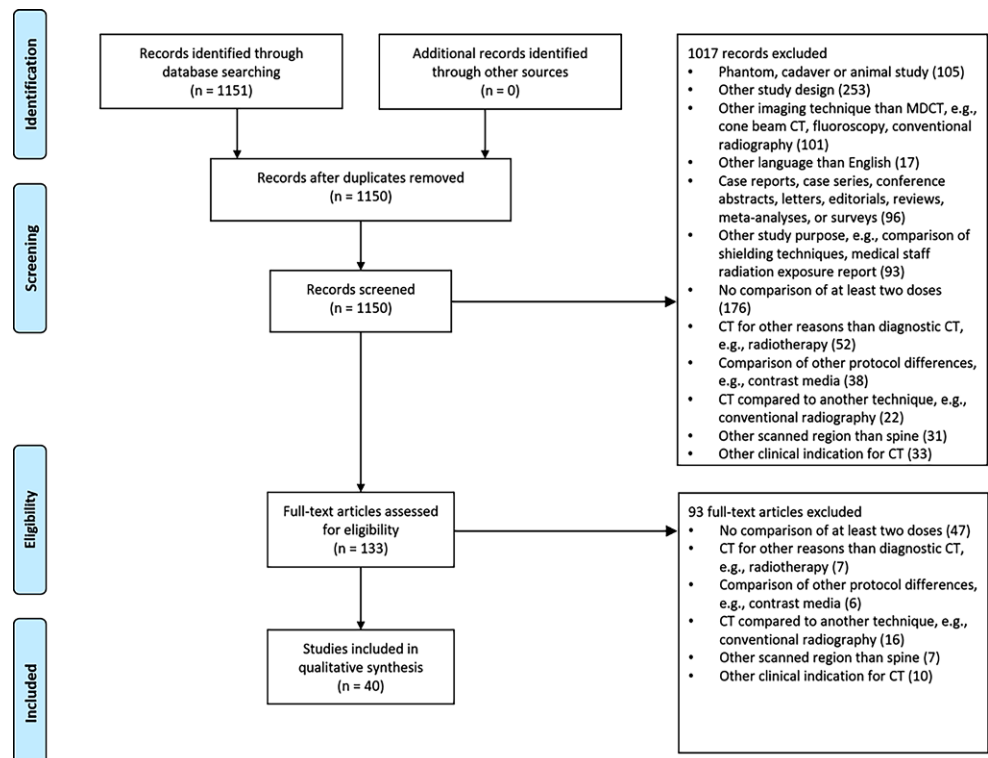
The following basic information was extracted: (1) author(s); (2) year of publication; (3) number of subjects (*n*) of the entire study and relevant patient subgroups (e.g., SD group, LD group); (4) scanned spine region, type of intervention (if applicable); (5) details on group comparisons (if applicable); (6) details on the used CT system, including number of detector rows, vendor, and model name; (7) image acquisition parameters; (8) image reconstruction algorithms and parameters; (9) dose reduction (in %) and reported dose values: CT dose index ($CTDI_{vol}$), dose length product (DLP), and/or effective dose (E).

Results

Study Selection

The search via PubMed resulted in 1150 publications after removal of duplicates (Fig. 1). During screening of titles and abstracts, 1017 records were discarded. The assessment of full-text articles led to the removal of 93 records, result-

Fig. 1 PubMed search flow diagram according to the preferred reporting items for systematic reviews and meta-analyses (PRISMA) guidelines [30, 31]. The used PubMed search terms are available in the appendix



ing in 40 publications that were included in the qualitative synthesis for this systematic review.

Study Characteristics

The 40 selected studies covered VF and spinal trauma ($n=14$), spinal degeneration ($n=6$), perioperative evaluation ($n=3$), and interventional spinal procedures ($n=17$).

Patients

The total number of subjects (n) as well as the number of subjects in the SD group(s) and LD group(s) were extracted when provided. Furthermore, the number of included CT examinations or subject numbers for relevant subgroups (e.g., CT scanner, BMI, preoperative/postoperative examination, fracture status, complication status) were extracted for some studies. Total numbers ranged from $n=20$ [32] to $n=380$ patients [33] and $n=1923$ CT examinations [34].

Scanned Spine Region

The most frequently covered region by CT imaging was the lumbar spine ($n=25$), followed by the cervical ($n=11$), thoracic ($n=4$), and sacral spine ($n=4$). Four studies included scans of the whole spine. CT examinations of sacroiliac joints and chest/abdomen/pelvis were counted as sacral spine and thoracic and lumbar spine, respectively.

CT System, Acquisition and Reconstruction Parameters

All studies included in this systematic review used multi-detector CT (MDCT). Tube voltages of 75–140 kV were used. In the majority of studies, LD protocols were built upon reduced tube currents, which were determined with different approaches: (i) fixed mA values or ranges, or (ii) reference mA values or ranges in the case of automated tube current modulation. Reporting of mA was heterogeneous, including reference values, mean or median values, and ranges. Statistics on the reported numbers would therefore not be meaningful to present. As an alternative or in addition to tube current, some studies reported tube current-time products, which take into account exposure time. The reported mAs values can be used as a measure of radiation exposure, in particular in CT-guided intervention studies.

Image reconstruction by FBP was reportedly used in 9 studies. Especially more recent studies used IR, which included hybrid IR (HIR), statistical IR (SIR), adaptive SIR (ASIR), and model-based IR (MBIR) ($n=21$). IR was used to create LD protocols and compared to SD protocols with FBP in six studies [35–40]. Reconstruction technique was not reported in 17 studies. As most of those studies were

published in 2017 or earlier, it is reasonable to assume that FBP was used.

Dose Reporting and Dose Reduction Calculation

Studies reported dose as $CTDI_{vol}$ ($n=27$), DLP ($n=29$), and E ($n=24$). Effective dose (E), commonly regarded as the most appropriate indicator of stochastic radiation risk, is derived by multiplying DLP with a conversion factor for a specific CT examination. Different DLP to E conversion factors were used from published studies, which depend on the scanned spine region, patient age, acquisition parameters, and time of publication. Not all studies used the same conversion factors, which ranged from 0.005 mSv/(mGy*cm) at the thoracolumbar spine to 0.020 mSv/(mGy*cm) at the cervical spine [41–49]. Five studies did not report conversion factors at all. As a result, E and dose reductions based thereon should be compared with caution.

Dose reductions were explicitly reported in 32 studies and retrospectively calculated from provided dose values in 5 studies, 2 studies reported dose reductions based on only $CTDI_{vol}$ [33, 50], 10 studies on only DLP [51–60], 7 studies on only E [34, 61–66], 5 studies on both $CTDI_{vol}$ and DLP [35–39], 1 study on both $CTDI_{vol}$ and E [67], and 1 study on both DLP and E [68]. Dose reduction was retrospectively calculated in one study based on only DLP [69], in two studies on only E [53, 70], and in another two studies on both $CTDI_{vol}$ and DLP [71, 72]. Achieved dose reductions ranged from 6% to 95%, not taking into account simulated LD studies. Simulation of LD data was performed in seven studies, either by virtually lowered tube currents [32, 73], sparse sampling using a reduced number of projections (Fig. 2; [74]), or both (Fig. 3; [75–77]).

Dose values were reported as mean (with or without standard deviation) or median (with or without minimum, maximum, and interquartile range). Only the mean was extracted when mean and median were provided. In Tables 1, 2, 3 and 4, dose values are provided for the SD group, LD group, and subgroups (e.g., scanned region, CT scanner, patient, size, BMI, preoperative/postoperative examination, proceduralist), where reasonably applicable.

Outcome Measures

Quantitative Measures

Quantitative outcome measures included physical metrics of objective image noise and contrast, as well as other quantitative parameters. A total of 16 studies reported on quantitative image noise, as standard deviation of Hounsfield units (HU) measured in a standardized region of interest (ROI) ($n=9$) or as signal-to-noise ratio (SNR) ($n=9$). Contrast-

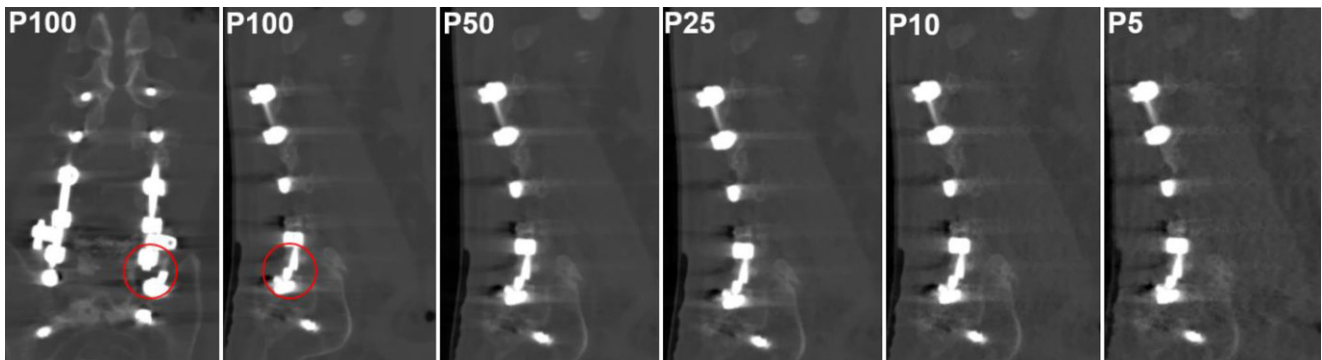


Fig. 2 Multidetector computed tomography (MDCT) images of a patient with implant failure after dorsal stabilization using a rod-screw system (spanning L1–S2). Coronal and sagittal MDCT reconstructions with statistical iterative reconstruction (SIR) are shown using 100% of projections (P100), and using sparse sampling with 50% (P50), 25% (P25), 10% (P10), and 5% (P5) of original projections. There is a left-sided rod defect (red circles) at the S1 level that is clearly depicted up to a dose reduction of at least 75% (P25)

to-noise ratio (CNR) was reported in five studies. Other quantitative parameters were reported in 18 studies: bone parameters (bone mineral density, bone fraction, trabecular number, trabecular separation, trabecular thickness, fractal dimension, finite element analysis, FEA-based failure load) for VF and spinal trauma; dural sac cross-sectional area for spinal degeneration; pedicle width and degree of vertebral rotation for perioperative evaluation; and procedure time and number of scans for interventional procedures.

Qualitative Measures

Purely quantitative outcome measures are important to enable a comparable IQ assessment [78]; however, more subjective outcome measures are needed to assess the utility of the images at different doses for the clinical application or diagnostic question. The most frequently reported qualitative measure comparable across all included studies were subjective IQ ($n=23$), containing common subcategories for some studies (overall IQ, overall artifacts, image contrast, sharpness, and depiction of certain spinal structures), followed by subjective utility or confidence for diagnosis or intervention planning ($n=12$) and subjective image noise ($n=4$). These measures usually used 3–5-point Likert scales. Furthermore, other application-specific variables were evaluated as outcome measures and are described in the corresponding sections. In 15 studies, qualitative items were rated by 2 or more readers, and interobserver agreement (IOA), assessed by intraclass correlation coefficient (ICC) or Cohen's kappa, was reported [79, 80]. Although IOA tended to be slightly lower for LD-CT, it remained at least substantial (>0.6) in most studies. Diagnostic performance for VF status or common degenerative changes was assessed in five studies, reporting classification metrics (accuracy, sensitivity, specificity; $n=3$) or area under the curve (AUC; $n=2$).

Dose Reduction in Vertebral Fractures and Spinal Trauma

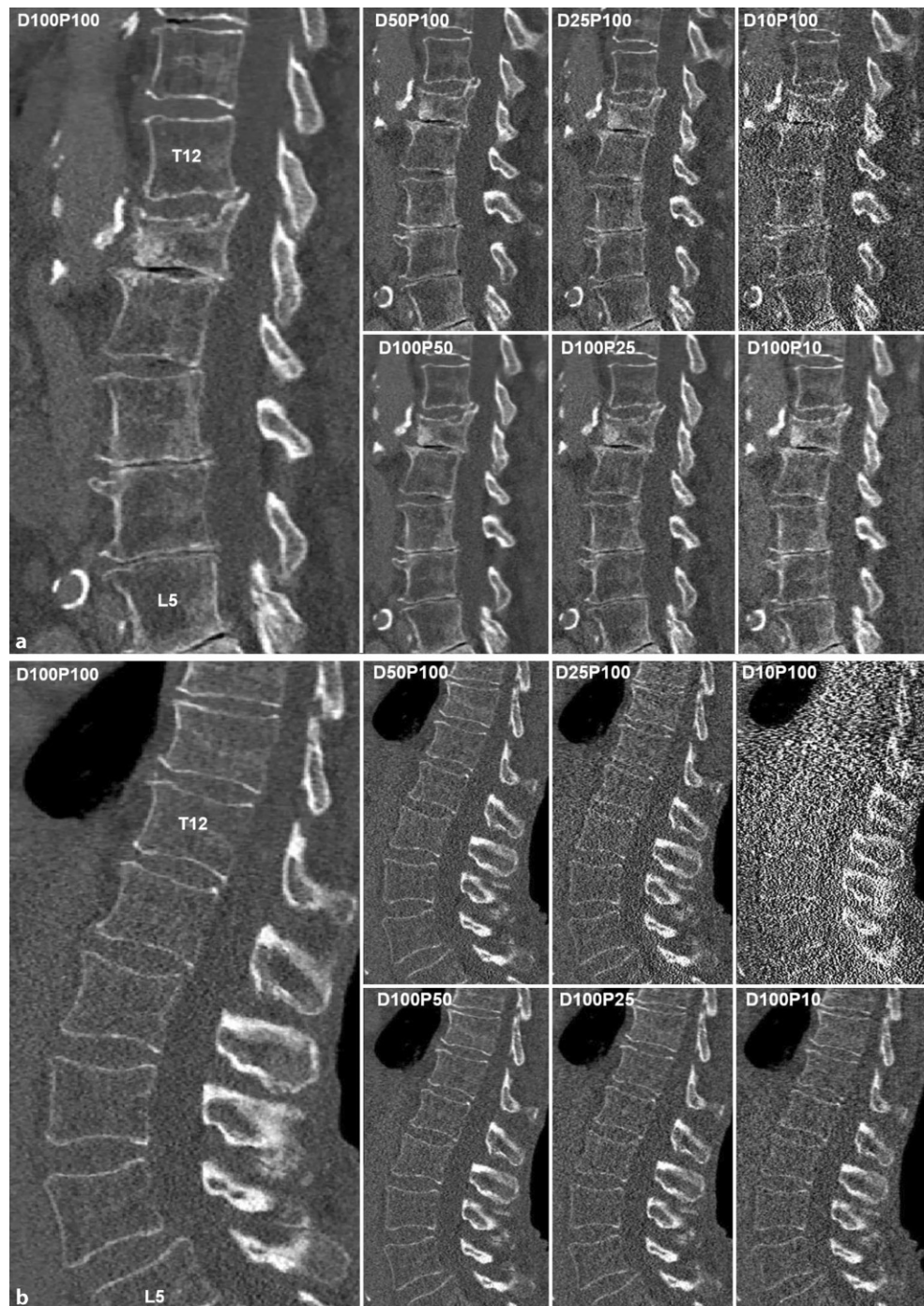
Vertebral fractures and spinal trauma were considered in 14 articles, including 7 studies which performed assessment of VF status [62–64, 67, 73, 75, 76], and were primarily performed at the thoracic or lumbar spine ($n=6$). One study reported on VF status of the cervical spine [67]. Studies without dedicated VF assessment focused on trauma of the cervical spine ($n=6$). One study from 2005, comparing optimized patient doses in single-slice CT (SSCT) and multi-slice CT (MSCT), was included and only results of lumbar spine scans were extracted [51]. Results are summarized in Table 1.

Vertebral Fracture Evaluation

Not taking into account simulated LD protocols, reported dose reductions ranged from 50% to 71% with preserved subjective IQ for VF detection (based on three studies [63, 64, 67]) and no effect on suggested treatment [64]. Reported doses in terms of $CTDI_{vol}$ and DLP ranged from 0.8 to 23.2 mGy and 188.4–403.7 $mGy \cdot cm$, respectively. The highest dose reduction of up to 71% was reported in 191 patients by Mulkens et al., who compared different SD and LD protocols using 2 different MDCT scanners [62].

The detection of VFs is an important indication of spinal CT. Good diagnostic performance as well as confidence for fracture detection and determination of fracture age were preserved for dose reductions up to 50% (Fig. 3), demonstrating high IOA [62, 64, 76]. Furthermore, the differentiation of patients with and without VF was investigated in four studies. Lee et al. reported sensitivity, specificity, and accuracy $\geq 95\%$ without significant differences between SD and LD [62, 64]. Two simulated LD studies demonstrated that quantitative bone parameters can reliably be assessed in LD-CT and found significant area under the curve (AUC)

Fig. 3 **a** Dose-reduced multi-detector computed tomography (MDCT) of the lower thoracic and lumbar spine in a 76-year-old patient with L1 fracture. Sagittal images were reconstructed using statistical iterative reconstruction (SIR) from original MDCT data using (i) full dose and 100% of projections (D100P100), (ii) tube current virtually reduced to 50, 25, and 10% (D50P100, D25P100, D10P100), and (iii) sparse sampling with only every second, fourth, or tenth projection (D100P50, D100P25, D100P10). **b** Dose-reduced multidetector computed tomography (MDCT) of the lumbar spine in a 74-year-old patient without vertebral fractures. Sagittal images were reconstructed using statistical iterative reconstruction (SIR) from original MDCT data using (i) full dose and 100% of projections (D100P100), (ii) tube current virtually reduced to 50, 25, and 10% (D50P100, D25P100, D10P100), and (iii) sparse sampling with only every second, fourth, or tenth projection (D100P50, D100P25, D100P10)



values in receiver operating characteristics (ROC) analysis, which could particularly benefit osteoporosis patients. Mei et al. reported an AUC of up to 0.9 without significant differences in bone mineral density (BMD) and certain bone microstructure parameters down to 10% of the SD (Fig. 3; [75]). Using FEA-based failure load, Anitha et al. reported an AUC of 0.7 without a significant difference down to 25% of the SD [73].

Spinal Trauma

Studies without dedicated VF assessment reported dose reductions ranging from 6% in 380 patients [33] to 55% in 147 patients [36] without a difference in subjective IQ (based on 7 studies [33, 35–37, 51, 61, 65]) and comparable image noise (based on 3 studies [36, 37, 65]). Reported doses in terms of CTDI_{vol} and DLP ranged from 6.2–21.4 mGy and 156.4–560.0 mGy*cm, respectively, not

Table 1 Dose reduction in vertebral fractures and spinal trauma

Author	Year	Subjects (n)	Scanned region	Comparison	CT System	Acquisition parameters	Reconstruction (name, level)	Dose reduction	CTDI _{vol} [mGy]	DLP [mGy*cm]	E [mSv]
Heggie [51]	2005	205 75 ^{SD} , MSCT 74 ^{LD} , MSCT 56 ^{CD} , SSCT	Lumbar	SD ^{MSCT} vs LD ^{MSCT} vs CD ^{SSCT}	SSCT (Siemens Somatom Plus 4) 16-MSCT (Siemens Sensation 16)	120 kVp, 360 mA ^s 120 kVp, 300 mA ^s 140 kVp	NA	20%	NA	560.0 ^{SD} 455.0 ^{LD} 455.0 ^{CD}	6.1 ^{LD}
Mulken [67]	2007	191 51 ^{SD} 140 ^{LD}	Cervical	SD vs LD 6-MDCT vs. 16-MDCT	6-MDCT (Siemens Emotion 6) 16-MDCT (Siemens Sensation 16)	130 kV, 175 mA ^s 120 kV, 250 mA ^s 110–130 kV ^{am} , LD, 6 100–120 kV ^{am} , LD, 16	NA	61–71%	23.2 ^{SD,6} 19.2 ^{SD,16} 15.3–23.2 ^{LD,6} 12.5–19.48 ^{LD,16}	NA	3.8 ^{SD} 1.1–1.6 ^{LD}
Maxfield [35]	2012	245 109 ^{SD} 136 ^{LD}	CAP BC	SD ^{FBP} vs. LD ^{ASIR}	64-MDCT (GE Lightspeed VCT)	NA	FBP ASIR	20% CTDI, DLP	17.1 ^{SD} , CAP 14.2 ^{LD} , CAP 61.7 ^{SD} , BC 49.6 ^{LD} , BC	1165.0 ^{SD} , CAP 1004.0 ^{LD} , CAP 1327.0 ^{SD} , BC 1067.0 ^{LD} , BC	19.8 ^{SD} , CAP 17.1 ^{LD} , CAP
Geyer [36]	2013	147 67 ^{SD} 80 ^{LD}	Cervical	SD ^{FBP} vs LD ^{ASIR}	64-MDCT (GE Lightspeed VCT XT) ^{SD} 64-MDCT (GE Discovery HD 750) ^{LD}	120 kV, max. 300 mA ^s	FBP ASIR (30%)	55% CTDI 54% DLP	21.4 ^{SD} 9.6 ^{LD}	441.2 ^{SD} 204.2 ^{LD}	2.4 ^{SD} 1.1 ^{LD}
Ardley [61]	2013	60 30 ^{rDA} 30 ^{sDA} 30 ^{sA}	BC	rDA vs sDA vs SA	128-MDCT (Philips Ingenuity)	120 kV ^{am}	NA	16%	919.3 ^{sDA,c} 813.1 ^{rDA,c}	1829.0 ^{rDA,t} 1735.6 ^{sDA,t} 1458.7 ^{sA,t}	3.4 ^{sA,t} 4.0 ^{sDA,t} 4.2 ^{rDA,t}
Mueck [33]	2014	380 126 ^{SD} , STD 254 ^{LD} , SWIM	Cervical	SD ^{SWIM} vs LD ^{STD}	64-MDCT (GE Discovery HD 750)	120 kV, 20–300 mA ^{am}	ASIR (30%)	6%	6.6 ^{SD} 6.2 ^{LD}	NA	0.8 ^{SD} 0.7 ^{LD}
Patro [37]	2016	78 48 ^{SD} , FBP 30 ^{LD} , ASIR	Cervical	SD ^{FBP} vs LD ^{ASIR}	64-MDCT (GE Lightspeed)	120 kV, 100–650 mA ^s 120 kV, 81–451 mA ^s	FBP ASIR (30%)	36%	16.8 ^{SD} 10.7 ^{LD}	404.5 ^{SD} 256.6 ^{LD}	2.4 ^{SD} 1.5 ^{LD}
Mei [75]	2017	24 12 ^{VF} 12 ^{rVF}	Thoracic Lumbar	SD vs LD ^{S1}	256-MDCT (Philips iCT)	120 kV, 200–400 mA ^s 109 mA ^s 11–55 mA ^s	SIR	50–90%	7.5 ^{SD} 0.8–3.8 ^{LD}	NA	NA
Lee [62]	2017	263 126 ^{SD} 137 ^{LD}	Lumbar	SD vs LD ^{BMI}	64-MDCT (Philips Ingenuity)	120 kV, 200–300 mA ^s 120 kV, 80–150 mA ^s	HIR (iDose 4)	47–69%	11.9 ^{SD} 6.2 ^{LD}	350.5 ^{SD} 188.4 ^{LD}	4.9 ^T , (3.6/4.7/5.7 ^{BMI}) ^{SD} 2.1 ^T , (1.1/2.0/3.0 ^{BMI}) ^{LD}

Table 1 (Continued)

Author	Year	Subjects (n)	Scanned region	Comparison	CT System	Acquisition parameters	Reconstruction (name, level)	Dose reduction	CTDI _{vol} [mGy]	DLP [mGy*cm]	E [mSv]
Weinrich [63]	2018	80 40 ^{SD} 40 ^{LD}	Lumbar	SD vs LD	256-MDCT (Philips Brilliance iCT)	120kV, 158 mAs ^f SD 140kV, 70 mAs ^f LD	HIR (iDose 3 ^{SD} , 4 ^{LD} , 6 ^{LD})	50% ^E	11.4 ^{SD} 6.9 ^{LD}	403.7 ^{SD} 209.2 ^{LD}	6.2 ^{SD} 3.2 ^{LD}
Lee [64]	2018	144 76 ^{SD} 68 ^{LD}	Lumbar	SD vs LD	320-MDCT (Toshiba Aquilion ONE dynamic volume CT)	120kVp, 200–300 mAs ^{am} SD 120kVp, 80–150 mAs ^{am} LD	MBIR (AIDR)	61% ^E	NA	NA	5.4 ^{SD} 2.1 ^{LD}
Anitha [73]	2019	16 8 ^{VF} 8 ^{nVF}	Lumbar	SD vs LD ^{S2}	256-MDCT (Philips iCT)	120kV, 200–400 mAs 112 mAs ^{SD} 11–56 mAs ^{LD}	FBP	50–90%	7.7 ^{SD} 0.8–3.8 ^{LD}	NA	NA
Sollmann [76]	2019	35 23 ^{VF} 12 ^{nVF}	Whole spine	SD vs LD ^{S1}	64-MDCT (Philips Brilliance 64)	120kV, 143 mA, 180 mAs ^{am} SD 18–90 mAs ^{LD}	FBP	50–90%	11.7 ^{SD} 1.2–5.9 ^{LD}	NA	NA
Toza-kidou [65]	2019	68 34 ^{SD} 34 ^{LD}	Cervical	SD vs LD	128-MDCT (Siemens Somatom Definition AS+)	120kV, 195 mAs ^{SD} 120kV, 105 mAs ^{LD}	IR (SAFIRE 3)	51% ^E	14.1 ^{SD} 7.0 ^{LD}	319.7 ^{SD} 156.4 ^{LD}	1.6 ^{SD} 0.8 ^{LD}

^{am} automatic tube current modulation, ^{BMI} BMI < 23/23–25/≥ 25 kg/m², ^c cervical spine dose, ^{CD} comparison dose of SSCT, ^{CTDI} based on CTDI_{vol}, ^E based on effective dose, ^{LD} low dose, ^{nVF} no vertebral fracture, ^r reference mAs value, ^{rDA} retrospective data acquired with dual acquisition technique, ^{SA} single acquisition technique, ^{SD} standard dose, ^{sDA} simulated dual acquisition data acquired with single acquisition technique, ^{STD} standard position, ^{swm} swimmer's position, ^{S1} 10/25/50% of SD using simulated lower tube currents and sparse sampling, ^{S2} 10/25/50% of SD using simulated lower tube currents, ^T all subjects, ^{VF} vertebral fracture, ⁶ 6-row-MDCT, ¹⁶ 16-row-MDCT
^{AIDR} adaptive iterative dose reduction, ^{ASIR} adaptive statistical iterative reconstruction, ^{BC} cervical spine and brain scan, ^{CAP} chest, abdomen and pelvis scan, ^{FBP} filtered back projection, ^{MBIR} model-based iterative reconstruction, ^{MDCT} multi-detector CT, ^{MSCT} multi-slice CT, ^{NA} not available, ^{SAFIRE} sinogram-affirmed iterative reconstruction, ^{SIR} statistical iterative reconstruction, ^{SSCT} single-slice CT

Table 2 Dose reduction in degenerative spine disease

Author	Year	Subjects (n)	Scanned region	Comparison	CT System	Acquisition parameters	Reconstruction (name, level)	Dose reduction	CTDI _{vol} [mGy]	DLP [mGy*cm]	E [mSv]
Bohy [81]	2007	60 8/37/15 ^{BMI1}	Lumbar	SD vs LD ^{S1}	4-MDCT (Siemens Somatom Volume Zoom)	140 kV, 200/300/400 ^{BMI1} mA _s ^{SD}	NA	35–80%	40.0 ^{SD,a}	NA	NA
Yang [38]	2014	164 50 ^{SD} 58 ^{LD1} 56 ^{LD2}	Lumbar	SD vs LD1 vs LD2	256-MDCT (Philips Brilliance iCT)	120 kV, 300 mA _s ^{am} SD 120 kV, 150 mA _s ^{am} LD1 100 kV, 230 mA _s ^{am} LD2	FBP ^{SD} HIR (iDose 4) ^{LD}	36% ^{CTDI,LD1} 47% ^{DLP,LD1} 60% ^{CTDI, DLP,LD2}	18.4 ^{SD} 10.0 ^{LD1} 7.3 ^{LD2}	587.5 ^{SD} 312.6 ^{LD1} 233.2 ^{LD2}	6.5 ^{SD} 3.4 ^{LD1} 2.6 ^{LD2}
Yang [39]	2016	113 55 ^{SD} 58 ^{LD}	Lumbar	SD vs LD ^{HIR} vs LD ^{IMR}	256-MDCT (Philips Brilliance iCT)	120 kV, 262 mA _s ^{am} SD 120 kV, 129 mA _s ^{am} LD	FBP ^{SD} HIR (iDose 4) ^{LD} MBIR (IMR 1) ^{LD}	49%	17.7 ^{SD} 8.7 ^{LD}	580.5 ^{SD} 283.4 ^{LD}	6.4 ^{SD} 3.1 ^{LD}
Iyama [40]	2017	34	Lumbar	FBP vs IMR vs HIR	256-MDCT (Philips Brilliance iCT)	120 kV, 127 mA ^{am}	FBP MBIR (IMR 1) MBIR (IMR 1) HIR (iDose 4) MRI ^m	NA	15.6	227.8–743.2	NA
Lee [52]	2017	260 143 ^{LD} 117 ^{ULD}	Lumbar	LD vs ULD ^{BMI2}	64-MDCT (Philips Ingenuity)	120 kV, 150 mA _s ^{LD} 120 kV, 30 mA _s ^{ULD}	IR	60–68%	7.7 ^{LD} 1.9 ^{ULD}	248.4 ^{LD} 60.5 ^{ULD}	2.9 ^{LD} 1.5/2.5/4.2 ^{BMI2,LD} 0.7 ^{T,ULD} 0.6/0.7/0.8 ^{BMI2,ULD}
Sollmann [77]	2021	26	Cervical Lumbosacral	SD vs LD ^{S2}	128-MDCT (Philips Ingenuity Core)	120/140 kV, 322 mA, 95 (130–314) mA _s ^{am} SD 6–98 mA _s ^{am} LD	SIR	50–97%	13.8 ^{SD} 0.4–6.9 ^{LD}	388.9 ^{SD}	NA

^{am} automatic tube current modulation, ^{BMI1} BMI < 22/22–30/≥ 30 kg/m², ^{BMI2} BMI < 23/23–25/≥ 25 kg/m², ^{CTDI_{vol}} based on CTDI_{vol}, ^{DLP} based on DLP, ^{LD} low dose, ^{LD1} low dose using 120 kV and 150 mA_s, ^{LD2} low dose using 100 kV and 230 mA_s, ^m as standard of reference, ^{S1} 20/35/50/65% of SD using simulated lower tube currents, ^{S2} 3/5/10/50% of SD using simulated lower tube currents and sparse sampling, ^{SD} standard dose, ^T all subjects corresponding to a standardized body represented by the Monte Carlo model ^{FBP} filtered back projection, ^{HIR} hybrid iterative reconstruction, ^{IMR} iterative model reconstruction, ^{IR} iterative reconstruction, ^{MBIR} model-based iterative reconstruction, ^{MDCT} multi-detector CT, ^{MRI} magnetic resonance imaging, ^{NA} not available, ^{SIR} statistical iterative reconstruction

Table 3 Dose reduction in perioperative evaluation

Author	Year	Subjects (n)	Scanned region	Comparison	CT System	Acquisition parameters	Reconstruction (name, level)	Dose reduction	CTDIvol [mGy]	DLP [mGy*cm]	E [mSv]
Abul-Kasim [70]	2008	127 ^{SD}	Thoracic	SD vs	16-MDCT	120kV,	NA	95% ^E	10.1 ^{SD}	714.0 ^{SD}	13.09 ^{SD}
		113 ^{LD}	Lumbar	LD vs	(Siemens)	165 mAs ^{SD}	NA		0.5 ^{LD}	20.8 ^{LD}	0.37 ^{LD}
		15 ^{CD}		CD	SOMATOM Sensation)	120kV, 25 mAs ^{LD} 120kV, 60 mAs ^{CD}			13.0 ^C	24.0 ^C	0.43 ^C
Sensakovic [66]	2016	31	Thoracic	SD vs	128-MDCT	NA ^{SD}	NA ^{SD}	84–91% ^E	8.9/13.0 ^{BMI,pre,SD}	402.7/599.6 ^{BMI,pre,SD}	7.5/10.7 ^{BMI,pre,SD}
		17 ^{SD}	Lumbar	LD	(Philips)	100kV,	HIR		14.1/11.9 ^{BMI,po,SD}	553.5/429.5 ^{BMI,po,SD}	10.5/8.1 ^{BMI,po,SD}
		17 ^{LD}			Ingenuity (Core)	25/40 ^{BMI,mAs} ^{LD}	(iDose 5) ^{LD}		1.0/1.6 ^{BMI,pre,LD} 0.1/1.6 ^{BMI,po,LD}	53.1/74.8 ^{BMI,pre,LD} 46.1/77.8 ^{BMI,po,LD}	1.0/1.4 ^{BMI,pre,LD} 0.9/1.3 ^{BMI,po,LD}
Sollmann [74]	2021	38	Whole spine	SD vs	128-MDCT	120–140kVp,	SIR	50–95%	12.6 ^{SD}	NA	NA
		24 ^{PC}		LD ^S	(Philips)	288 mAs,			0.6/1.3/3.2/6.3 ^{S,LD}		
		14 ^{nc}			Ingenuity (Core)	148 mAs ^{am,SD}					

^{am} automatic tube current modulation, ^{BMI} BMI $\leq 25\text{ kg/m}^2\text{, CD}$ comparison dose based on older CT protocol for surgery planning, ^E based on effective dose, ^{LD} low dose, ^{nc} no postoperative complications, ^{PC} postoperative complications, ^{PO} postoperative, ^{pre} preoperative, ^S 5/10/25/50% of SD using simulated sparse sampling, ^{SD} standard dose HIR hybrid iterative reconstruction, ^{MDCT} multi-detector CT, ^{NA} not available, ^{SIR} statistical iterative reconstruction

taking into account examinations covering brain and cervical spine or chest, abdomen, and pelvis. In 2005, lumbar spine scans of SSCT and MSCT were compared and it was shown that protocol optimization of the newly introduced CT hardware might reduce dose by 20% to match SSCT levels [51]. Between 2012 and 2016, 3 studies compared ASIR to FBP for image reconstruction in a total of 470 patients, resulting in dose reductions between 20% (without delayed diagnoses or missed injuries) and 55%, underlining the importance of MDCT as the first-line imaging method for spinal trauma [35–37].

Beyond modulation of tube voltage or current, other approaches for dose reduction were investigated. Ardley et al. compared retrospective and simulated dual acquisitions (DA; two single scans) of the brain and cervical spine to a single acquisition (SA) covering both anatomical regions. Due to the elimination of overscanning and overlap of the 2 regions, a total dose reduction of 16% with excellent diagnostic IQ could be achieved [61]. Mueck et al. compared the effect of different arm positions in 380 cervical trauma patients and found improved IQ at a dose reduction of 6% at the cervicothoracic junction for the swimmer’s position with an optimal shoulder girdle angle >10°, in particular for higher BMI [33]. Also investigating the lower cervical spine, Tozakidou et al. reported that dose can be reduced by 51% without IQ impairment by using an LD protocol in patients without superimposition of C5 and the shoulder girdle [65].

Dose Reduction in Degenerative Spine Disease

Degenerative spine disease was considered in six articles, including the evaluation of intervertebral discs (IVDs) (n=5 [38, 39, 52, 77, 81]) and other conditions, such as facet joint osteoarthritis, spondylosis, (pseudo)spondylolisthesis, and intervertebral foramen (IVF) narrowing. Patients with low back pain (LBP) were explicitly investigated in two studies [39, 52]. Results are summarized in Table 2.

In the context of IVD evaluation, achieved dose reductions ranged from 35–97%. Using simulated reduced doses at 20–65% of the BMI-adapted tube charge presets, Bohy et al. found no significant effect on identification of bulging IVDs and IVF compromise, while identification of normal IVDs, spinal canal compromise (for $\leq 50\%$ of SD), and herniated IVDs (for $\leq 35\%$ of SD) was impaired. In this study, no explicit patient dose values were obtained; however, a SD of 40.0mGy corresponding to a standardized body represented by Monte Carlo simulation was reported. The authors concluded that a dose reduction using 65% of SD could be achieved via modification of BMI-adapted tube charge for suspected lumbar disc disease (LDD) [81].

In two studies published in 2014 and 2016, Yang et al. compared FBP-reconstructed SD-CT with IR-reconstructed

Table 4 Dose reduction in interventional procedures

Author	Year	Subjects (n)	Scanned region	Intervention	Comparison	CT System	Acquisition parameters	Reconstruction (name, level)	Dose reduction	CTDI _{vol} [mGy]	DLP [mGy*cm]	E [mSv]
Shepherd [53]	2011	100 50 ^{SD} 50 ^{LD}	Whole spine	PRU/PI	SD vs LD	64-MDCT (GE Lightspeed VCT)	120 kV, 549 ^S /84 ^P /84 ^S /199 ^{PC} mA ^{SD} 120 kV, 149 ^S /30 ^P /50 ^S /50 ^{PC} mA ^{LD}	NA	86% ^{DLP} 90% ^{E,c} 81% ^{E,l}	NA	1458.0 ^{SD} 199 ^{LD}	9.7 ^{c,SD} 17.5 ^{l,SD} 1.1 ^{c,LD} 3.3 ^{l,LD}
Schaubberger [82]	2012	80	Lumbar	PRU/PI	Proceduralist ^{pr} Patient habitus ^{dia}	16-MDCT (GE Lightspeed)	120 kV, 100–440 mA ^{am p} 120 kV, 66/42/49/80 mA ^{pr,g}	NA	NA	88/34/ 79/149 ^{pr}	NA	NA
Artner [34]	2012	1923 1870 ^{SD} 53 ^{LD}	Lumbar	PRU/PI	SD vs LD	16-MDCT (Siemens SOMATOM Emotion)	130 kV, 120 ^S /80 ^P /50 ^S mA ^{SD} 80 kV, 100 ^S /80 ^P /50 ^S mA ^{LD}	NA	85%	NA	NA	1.49 ^{SD} 0.22 ^{LD}
Artner [54]	2012	100 50 ^{SD} 50 ^{LD}	Lumbar	PRU/PI	SD vs LD	16-MDCT (Siemens SOMATOM Emotion)	130 kV, 120 ^S /80 ^P /50 ^S mA ^{SD} 80 kV, 100 ^S /80 ^P /50 ^S mA ^{LD}	NA	85% ^{no}	NA	94.4 ^{SD} 13.9 ^{LD}	NA ^{SD} 0.2 ^{LD}
Artner [55]	2012	65 5 ^{SD,ctg} 30 ^{LD,ctg} 30 ^{flg}	Sacral	PRU/PI	SD vs LD	16-MDCT (Siemens SOMATOM Emotion)	130 kV, 120 ^S /80 ^P /50 ^S mA ^{SD,ctg} 80 kV, 50 ^S mA ^{LD,ctg} 75–80 kV, 60 mA ^{flg}	NA	94%	NA	76.3 ^{SD,ctg} 4.6 ^{LD,ctg} 3.7 ^{fl}	NA
Paik [56]	2014	247 124 ^{SD} 123 ^{LD}	Lumbar	PRU/PI	SD ^{hep} vs LD ^{sep}	16-MDCT (GE Brightspeed Elite)	120 kV, 10 ^S /50 ^P /30 ^S mA ^{SD,hep} 120 kV, 10 ^S /30 ^P /30 ^S mA ^{SD,sep}	NA	85%	NA	31.8 ^{SD} 4.9 ^{LD}	0.5 ^{SD} 0.09 ^{LD}
Shpilberg [71]	2014	64 35 ^{SD} 29 ^{LD}	Whole spine	Biopsy	SD vs LD	4-MDCT (Siemens Volume Zoom) 8-MDCT (GE Lightspeed Ultra)	120 kV, >200 mA ^{s SD} 80 kV, 40–60 mA ^{s LD}	NA	76% ^{CTDI} 61% ^{DLP}	285.2 ^{SD} 69.5 ^{LD}	1541.0 ^{SD} 601.5 ^{LD}	NA
Paik [57]	2015	338 163 ^{SD} 175 ^{LD}	Cervical	PRU/PI	SD ^{hep} vs LD ^{sep}	16-MDCT (GE Brightspeed Elite)	120 kV, 10 ^S /50 ^P /40 ^S mA ^{SD,hep} 120 kV, 10 ^S /40 ^P /40 ^S mA ^{LD,sep}	NA	80%	NA	39.1 ^{SD} 7.9 ^{LD}	0.5 ^{SD} 0.1 ^{LD}

Table 4 (Continued)

Author	Year	Subjects (n)	Scanned region	Intervention	Comparison	CT System	Acquisition parameters	Reconstruction (name, level)	Dose reduction	CTDI _{vol} [mGy]	DLP [mGy*cm]	E [mSv]
Amrhein [58]	2016	80 40 ^{SD} 40 ^{LD}	Lumbar	PRU/PI	SD vs LD	16-MDCT (GE Lightspeed)	120 kV, 435(100–440) ^P mA ^{am,SD} 120 kV, 68(50–100) ^P mA ^{LD}	NA	78% ^{DLPi}	39.1 ^{P,SD} 4.2 ^{P,LD}	432.1 ^{LD} 313.1 ^{P,SD} 94.2 ^{LD} 27.9 ^{P,LD}	NA
Greffier [50]	2017	602 162 ^{SD} 440 ^{LD}	Lumbar	PRU/PI Vertebral expansion Biopsy	SD vs LD	64-MDCT (Siemens SOMATOM Definition AS+)	120 kV, 275 ^{hm} /60 ^{fm} /60 sm mA ^{s,r,SD} 100 ^{hm} /80 ^{fm} /80 sm kV, 200 ^{hm} /60 ^{fm} /60 sm mA ^{s,r,LD}	FBP	58% ^{hm} 72% ^{fm} 72% sm	18.3 ^{hm,SD} 9.2 ^{fm,SD} 5.1 ^{sm,SD} 7.9 ^{hm,LD} 2.6 ^{fm,LD} 1.5 ^{sm,LD}	NA	NA
Eisholtz [68]	2017	85 22 ^{SD} 63 ^{LD}	Lumbar	PRU/PI	SD ^{kep} vs LD ^{scp}	80-MDCT (Toshiba Aquilion PRIME)	120 kV, 20 ^P /20 ^S mA ^{s,SD} 100 kV, 10 ^P /5 ^S mA ^{s,LD}	NA	64%	NA	8.9 ^{SD} 3.2 ^{LD}	0.048 ^{SD} 0.014 ^{LD}
Eisholtz [83]	2017	79 183 ^P	Lumbar	PRU/PI	ULD ^{BMI}	80-MDCT (Toshiba Aquilion PRIME)	100 kV, 5 mA ^s	IR (AIDR)	NA	NA	2.4/23/3.4 ^{BMI}	0.05/0.05 /0.07 ^{BMI}
Eisholtz [59]	2019	183 101 ^{SD} 82 ^{LD}	Cervical	PRU/PI	SD ^{kep} vs LD ^{scp}	64-MDCT (Siemens SOMATOM Definition) ^{SD} 80-MDCT (Toshiba Aquilion PRIME) ^{LD}	100 ^P /100 ^S kV ^p , NA ^{am,p} /28 ^S mA ^{s,SD} 100 ^P /80 ^S kV ^p , 10 ^P /5 ^S mA ^{s,LD}	FBP ^{SD} IR (AIDR) ^{LD}	93%	NA	22.0 ^{P,SD} 1.7 ^{S,SD} 24.3 ^{LD} 0.8 ^{P,LD} 1.0 ^{S,LD} 1.8 ^{LD}	0.14 ^{LD,SD} 0.01 ^{LD}
Sollmann [32]	2019	20	Lumbosacral	PRU/PI	SD vs LD ^{SI}	128-MDCT (Philips Ingenuity Core)	120 kV, 133 mA, 100 mA ^{s,P,SD} 120 kV, 1–50 mA ^{s,P,SD}	SIR (A) SIR (B)	50–99%	6.5 ^{SD} 0.07–3.3 ^{LD}	26.0 ^{SD} 0.3–13.0 ^{LD}	NA

Table 4 (Continued)

Author	Year	Subjects (n)	Scanned region	Intervention	Comparison	CT System	Acquisition parameters	Reconstruction (name, level)	Dose reduction	CTDI _{vol} [mGy]	DLP [mGy*cm]	E [mSv]
Cordts [72]	2020	64 ^{pro}	Lumbo-sacral	LP	SD vs LD	128-MDCT (Philips Ingenuity Core)	120 kV, 133 mA, 100 mAs ^{SD}	HIR	69% ^{CTDI}	6.5 ^{SD}	58.0 ^{SD}	NA
		20 ^{pro,LD}					120 kV, 40 mA, 30 mAs ^{LD}	4) ^{SD}	83% ^{DLP}	2.0 ^{LD}	10.0 ^{LD}	
		13 ^{pat}						MBIR (IMR) ^{LD}				
Rosiak [69]	2021	65 ^{pro}	Lumbar	LP	SD vs LD	MDCT (Toshiba/Canon Aquilion One)	120 kV, 100 mA ^{SD}	NA	89%	NA	248.1 ^{SD}	NA
		23 ^{pro,SD}					120 kV, 10 mA ^{LD}				26.7 ^{LD}	
		42 ^{pro,LD}										
	18 ^{pat}											
Paprottka [60]	2022	204	Cervical Lum-bosacral	PRI	SD vs LD	128-MDCT (Philips Ingenuity Core)	120 kV, 40 mA, 30 mAs ^{SD}	MBIR (IMR)	34% ^{DLP}	2.0 ^{pro,SD}	10.2 ^{pro,SD}	NA
		102 ^{SD}								1.8 ^{pro,LD}	6.8 ^{pro,LD}	
		102 ^{LD}					120 kV, 20–30 mA, 15–20 mAs ^{LD}					

^{am} automatic tube current modulation, ^{BMI} BMI < 25/25–30/≥ 30 kg/m², ^c cervical spine, ^{CTDI} based on CTDI_{vol}, ^{ctg} CT-guided, ^{dia} anterior-posterior diameter subgroups: <20/20–30/>30 cm, ^E based on effective dose, ^{fig} fluoroscopy-guided, ^{fin} fluoroscopy mode, ^g guide phase, ^{hsp} helical CT for planning, ^{hm} helical mode, ^l lumbar spine, ^{LD} low dose, ^{no} non-obese patients, ^p planning phase, ^{pat} number of patients, ^{pc} post contrast images, ^{pr} subgroups by performing proceduralist: 2/8/15/15 years of experience, ^{pro} number of procedures, ^r reference mAs value, ^{s1} 1/5/10/50% of SD using simulated lower tube currents, ^s survey, ^{SD} standard dose, ^{sep} spot CT for planning, ^{sl} scan length, sm sequential mode, ^t total procedure, ^{tp} total number of procedures, ^{AIDR} adaptive iterative dose reduction, ^{ASIR} adaptive statistical iterative reconstruction, ^{FBP} filtered back projection, ^{HIR} hybrid iterative reconstruction, ^{IMR} iterative model reconstruction, ^{IR} iterative reconstruction, ^{LP} lumbar puncture, ^{MBIR} model-based iterative reconstruction, ^{MDCCT} multi-detector CT, ^{NA} not available, ^{PRI/PI} periradicular infiltration or pain injection, ^{SIR} statistical iterative reconstruction

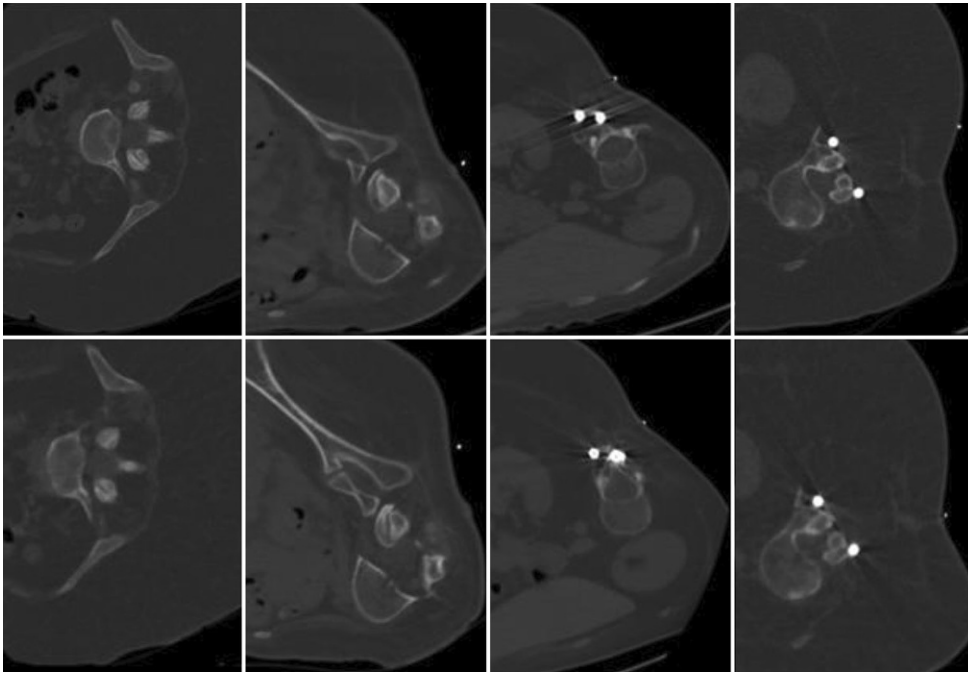


Fig. 4 Standard dose (SD; *upper row*) and low dose (LD; *lower row*) multi-detector computed tomography (MDCT) scans for procedure planning of intrathecal nusinersen administration in four patient cases with spinal muscular atrophy (SMA). Tube current was reduced from 133 mA in SD scans to 20, 40, 67 and 27 mA, in LD scans, resulting in considerable dose reductions. The SD scans were reconstructed using hybrid iterative reconstruction (iDose⁴; Philips Healthcare, Best, The Netherlands) while the LD scans were reconstructed using model-based iterative reconstruction (IMR; Philips Healthcare, Best, The Netherlands). The LD images demonstrate a blurrier appearance, but the reduced image quality of the LD scans did not impair the confidence for intervention planning. Due to the model-based iterative reconstruction, the LD images show less streak artifacts from metal implants (third and fourth column)

LD-CT of the lumbar spine and achieved dose reductions of 36–60% [38, 39]. For LD, an intended dose reduction of 50% was realized using two approaches, pure tube current reduction and simultaneous tube voltage and current reduction, which were both combined with HIR. Subjective IQ, SNR, and IOA were equivalent to SD for IVDs and the majority of the other analyzed anatomic regions for the first approach, while SNR, CNR, and IOA were inferior for the second method [38]. In terms of overall diagnostic acceptability, SNR and CNR, LD-CT with knowledge-based iterative model reconstruction (IMR) appeared to be non-inferior to LD-CT with HIR as well as FBP-reconstructed SD-CT. Furthermore, knowledge-based IMR yielded good IOA for IVD conditions [39].

Lee et al. compared LD-CT to ultralow dose (ULD)-CT of the lumbar spine in 260 LBP patients. Despite lower SNR, ULD showed high IOA with respect to IQ and final diagnosis. In non-obese patients, there was no significant difference in diagnostic performance for LDD [52]. Sollmann et al. investigated virtual LD-CT of the cervical and lumbosacral spine by using simulated tube current reduction or a reduced number of acquired projections [77]. Unsurprisingly, subjective IQ and contrast decreased with virtual dose reduction; however, all degenerative changes under investigation could be detected correctly down to 50% of the

standard tube current or number of projections. At higher dose reduction (10% of SD), virtual tube current reduction resulted in frequently missed non-calcified disc herniations, in contrast to sparse-sampled LD which still allowed for correct identification of all degenerative changes. Sparse sampling may therefore have higher potential for further dose reduction in the future.

Using magnetic resonance imaging (MRI) as reference standard, Iyama et al. investigated IQ and interobserver reliability of lumbar spinal CT using different reconstruction techniques [40]. Of note, dural sac cross-sectional area was calculated representing a quantitative parameter that was not used in other studies included in this review. Compared to HIR and FBP, IMR demonstrated higher subjective and objective IQ, higher IOA of spinal stenosis, and narrower limits of agreement in Bland-Altman analysis. The reported dose ($CTDI_{vol}=15.6\text{ mGy}$; $DLP=227.8\text{--}743.2\text{ mGy}\cdot\text{cm}$) was in the range of SD values of the other degenerative spine disease studies ($CTDI_{vol}=7.7\text{--}18.4\text{ mGy}$; $DLP=248.4\text{--}587.5\text{ mGy}\cdot\text{cm}$).

Dose Reduction in Perioperative Evaluation

Perioperative evaluation was considered in three articles, including pediatric spinal surgery for adolescent idiopathic

Table 5 Protocol recommendations and reference radiation dose levels

	Tube voltage [kV]	Tube current time product range [mAs]	CTDI _{vol} [mGy]	DLP [mGy*cm]	Reconstruction	Additional considerations
Vertebral fractures and spinal trauma	120	55–105 with ATCM	6–11	204–254	State of the art IR: ASIR, HIR or MBIR	Different arm positions available for cervical spine scans
Degenerative spine disease	120–140	30–150 with ATCM	2–10	61–313	State of the art IR: MBIR better than HIR	Use higher (effective) tube current time product for high BMI patients to maintain sufficient image quality
Interventional procedures	60–120	5–50 without ATCM	2–10 ^a	2–94 ^a	Use state-of-the-art IR over FBP if available	Optimize acquisition parameters for each phase of the procedure: Survey, planning, guide phase and postcontrast images Spot scanning better than helical scanning for planning images Sequential scanning better than helical scanning for guide phase images Reduce scanned area of interest as much as possible Set acquisition parameters according to patient habitus as scans are usually performed without ATCM
Achievable dose (reference)	–	–	17–25	362–531	–	–
Diagnostic reference level (reference)	–	–	23–33	495–703	–	–

ASIR adaptive statistical reconstruction, ATCM automatic tube current modulation, IR iterative reconstruction, HIR hybrid iterative reconstruction, MBIR model-based iterative reconstruction

^aDepending on phase of the procedure

scoliosis (AIS) ($n=2$) and patients with spinal instrumentation ($n=1$). Results are summarized in Table 3.

In the context of spinal surgery for AIS, the achieved dose reduction range of 84–95% without a relevant impairment of IQ. Abul-Kasim et al. compared 113 LD-CTs before and after surgical correction to SD-CT acquired in 127 trauma patients and sequential CTs acquired for surgery planning in 15 patients and concluded that LD spinal CT allows detailed preoperative planning and postoperative evaluation [70]. In a total of 31 pediatric patients, Sensakovic et al. additionally found that dose can be reduced to the level of 2-view radiography and depends on patient size and whether the scan is preoperative or postoperative [66].

To investigate the impact of sparse sampling and SIR on metal artifacts, Sollmann et al. applied simulated LD-CT in 38 patients with ($n=24$) and without complications ($n=14$) after spinal instrumentation by using 5, 10, 25, 50, or 100% of the acquired projections (P5, P10, P25, P50, P100) [74]. Although overall IQ decreased and artifacts increased with reduced number of projections, all complications were detected for P100, P50, and 25, and diagnostic confidence was high down to P25, and interreader agreement was substan-

tial to almost perfect. The authors concluded that 25% of the original projections might be still sufficient for detection of major instrumentation-related complications, which equals a 75% dose reduction (Fig. 2).

Dose Reduction in Interventional Procedures

Interventional procedures were considered in 17 articles. The majority focused on PRIs and other pain injections ($n=13$), mainly performed at the lumbar and cervical spine. Two articles investigated lumbar punctures (LPs) in spinal muscular atrophy (SMA) patients. Other procedures included spine biopsies and vertebral expansions. Specific outcome measures included procedure time, number of acquired scans and technical success, which were reported in 59% ($n=10$), 53% ($n=9$), and 53% ($n=9$) of the studies, respectively. Results are summarized in Table 4.

Periradicular Infiltrations and Other Pain Injections

Excluding LD simulations, reported dose reductions ranged from 34% in 204 PRI patients [60] up to 93% in 183 cervi-

cal PRI patients [59] and 94% in 65 sacroiliac joint injection patients [55]. The use of LD protocols did not meaningfully affect the rate of complications [54, 55, 58] or patient-reported pain [53, 59, 68].

CT-guided spinal interventions usually comprise different phases, which can include survey images, planning images, guide images during the procedure, and postcontrast images after the procedure, which all contribute to radiation exposure to the patient. Early studies in 2011 and 2012 used reduced tube voltages and currents to achieve very high dose reductions (81–94%) for different procedure phases without affecting technical success [34, 53–55]. Shepherd et al. achieved the major part of the dose reduction during the guide phase, using sequential axial acquisitions with short scan length instead of helical acquisitions [53]. Artner et al. accomplished a high portion of the dose reduction also in the survey and planning phase. Reducing the scanned area of interest in addition to tube voltage and current still provided sufficient IQ for technical success, although achievable dose reduction is more limited in obese patients [34, 54]. For sacroiliac joint injections, the authors replaced the survey image by palpation of anatomical landmarks, which reduced the dose to the levels of fluoroscopy, an alternative method regularly used for certain pain injections [55].

In addition to modified tube settings, the studies by Paik et al. and Elsholtz et al. used a spot scan instead of helical CT for planning, achieving dose reductions of 64–85% for lumbar and 80–93% for cervical injections [56, 57, 59, 68]. Only modifying the planning phase, Amrhein et al. achieved a dose reduction of 78% by reducing scan length and selecting a fixed tube current based on the body diameter of the patient in the survey scan [58].

Using virtually lowered tube currents in 20 PRI patients, Sollmann et al. found sufficient IQ to not affect confidence for intervention planning down to 10% of the SD [32]. After implementation of an LD protocol with tube currents reduced from 40 mA to 20–30 mA, a study in 204 patients observed no relevant difference in IQ or nerve root determination. The reported dose reduction of 34% did not affect the confidence for both planning and performing PRIs at the cervical and lumbosacral spine [60].

Two studies did not perform a dedicated SD to LD comparison; however, it was found that other factors can have a significant effect on tube settings as well as IQ, and hence dose [82]. Patient habitus had a greater influence than the performing interventionalist, which is in line with results from a ULD study that found increased doses only in patients with a BMI ≥ 30 kg/m² [83].

Lumbar Punctures in SMA Patients

Intrathecal nusinersen injection is an approved SMA treatment [84]. Patients frequently have severe scoliosis or spondylodesis, requiring CT-guided LP. Since the treatment is performed repeatedly, dose reduction is highly desirable. In 2 studies with 31 patients who underwent a total of 129 procedures dose reductions of 69–89% were found (Fig. 4). The higher dose reduction reported by Rosiak et al. was probably achieved by additional reduction of scan length along the spine [69]. All procedures were successful without increasing procedure time or requiring additional attempts to reach the intrathecal space [69, 72].

Other Interventions

CT-guided biopsy is the method of choice for the diagnosis of suspected spinal malignancy. At a dose reduction of 76%, Shpilberg et al. found no difference in the number of scans or procedure time for LD compared to SD protocol. Most importantly, diagnostic tissue yield with respect to malignancy and lesion type (lytic, sclerotic, or mixed) was not affected [71]. Investigating different spinal interventions, Greffier et al. found dose reductions of 58–72%. Highest reductions were achieved with sequential mode and fluoroscopy mode during the guide phase, which therefore should be used instead of helical scanning [50].

Protocol Recommendations and Recommended Radiation Dose Levels

Methodology and design of the included studies are heterogeneous. Therefore, it is difficult to make universal CT protocol recommendations; however, we derived recommendations for the most important parameters for reduced dose protocols in vertebral fractures and spinal trauma, degenerative spine disease and interventional procedures. For perioperative evaluation, not enough comparable studies were included to derive meaningful protocol recommendations. Table 5 summarizes the derived low dose protocol recommendations. Recommended radiation dose values derived from the studies included in this review were all lower than literature reference values. For comparison, achievable doses (AD) and diagnostic reference levels (DRL), defined as 50th and 75th percentile of recorded radiation doses, respectively, were extracted from [85] and [86]. These dose values are only reported for cervical spine scans and should therefore be referenced with care. Studies published before 2013 were not considered for protocol recommendations.

Discussion

In this article, dose reduction techniques for spinal CT were systematically reviewed. We included 40 studies representing the most common clinical indications. Comparison of LD and SD was most frequently performed between modified tube settings and reconstruction techniques.

For evaluation of VF and spinal trauma, achieved dose reductions ranged from 6–71%. The majority of studies reduced the dose by at least 50% while maintaining overall diagnostic performance and confidence. Besides tube settings and reconstruction techniques, patient positioning and decreasing overlapping scan regions were approaches to reduce exposure. For evaluation of degenerative spine disease, dose reductions without a negative effect on diagnostic performance and acceptable IQ range of 35–50%. Although not consistently investigated across all included studies, overall dose reduction potential tended to be higher for more advanced reconstruction techniques and nonobese patients. Highest dose reductions were achieved for perioperative evaluation and interventions. The reported values for perioperative evaluation ranged from 75% to 95% without negatively affecting the clinical value of the images. For interventional procedures, dose reductions ranged from 34% to 93%, largely depending on the dose reduction approach as well as type and targeted phase of the procedure. The majority of those studies even achieved a dose reduction of >70% while maintaining sufficient IQ for planning and guidance.

Dose reduction in spinal CT has in a large part been achieved by modifying tube settings while ensuring acceptable IQ using advanced reconstruction techniques. While these advances in LD-CT have been effectively enabled by new software, current and future developments in CT hardware will very likely increase dose reduction. Sparse-sampled CT enabled an additional dose reduction by a factor of 2 or more in simulation studies of the spine [71–74] as well as in other indications [87]. Clinical translation can be expected once the required X-ray tube technology is available for patient examinations [23]. Up to now, spinal applications of spectral CT have mainly been restricted to artifact reduction [88]. The clinical introduction of photon counting CT (PCCT) can be considered a new era for CT imaging, also with respect to radiation exposure [89, 90]. This innovative technology is expected to further improve IQ mainly due to reduction of electrical noise and artifacts, thus enabling dose reductions. Furthermore, it will potentially advance quantitative capabilities of spinal CT, such as more accurate BMD measurements and bone marrow quantification via material decomposition. Another emerging technique on the brink of clinical translation is AI which can be expected to bring additional dose reductions to spinal CT affecting both acquisition (e.g., via optimized patient

positioning or scan volume selection) and reconstruction (e.g., via CNNs trained on low-quality LD and high-quality SD data) [25–29].

In conclusion, considerable dose reduction in spinal CT can be realized by general approaches, such as tube setting modifications and advanced image reconstruction, but can be further increased through specific techniques for certain applications. Additional dose reduction up to 50% with comparable image quality can be expected from the clinical transition of novel acquisition and reconstruction techniques in the upcoming years.

Open Access This article is licensed under a Creative Commons Attribution 4.0 International License, which permits use, sharing, adaptation, distribution and reproduction in any medium or format, as long as you give appropriate credit to the original author(s) and the source, provide a link to the Creative Commons licence, and indicate if changes were made. The images or other third party material in this article are included in the article's Creative Commons licence, unless indicated otherwise in a credit line to the material. If material is not included in the article's Creative Commons licence and your intended use is not permitted by statutory regulation or exceeds the permitted use, you will need to obtain permission directly from the copyright holder. To view a copy of this licence, visit <http://creativecommons.org/licenses/by/4.0/>.

Appendix

PubMed Search Terms

Dose Reduction in Vertebral Fractures and Spinal Trauma

- ((computed tomography) OR (CT)) AND ((low-dose) OR (low dose) OR (dose reduction) OR (low-kilovolt) OR (low kilovolt) OR (low-kV) OR (low kV) OR (iterative reconstruction)) AND ((vertebral fracture) OR (spinal fracture) OR (vertebral trauma) OR (spinal trauma)).

Dose Reduction in Degenerative Spine Disease

- ((computed tomography) OR (CT)) AND ((low-dose) OR (low dose) OR (dose reduction) OR (low-kilovolt) OR (low kilovolt) OR (low-kV) OR (low kV) OR (iterative reconstruction)) AND ((degenerative spine) OR (spinal degeneration) OR (osteochondrosis) OR (spinal stenosis) OR (neuroforaminal stenosis) OR (scoliosis) OR (disc herniation) OR (disc protrusion) OR (degenerative disc disease) OR (facet arthropathy) OR (facet joint arthrosis)).

Dose Reduction in Perioperative Evaluation

- ((computed tomography) OR (CT)) AND ((low-dose) OR (low dose) OR (dose reduction) OR (low-kilo-

volt) OR (low kilovolt) OR (low-kV) OR (low kV) OR (iterative reconstruction)) AND ((postoperative spine) OR (dorsal stabilization) OR (ventral stabilization) OR (spinal instrumentation) OR (vertebral body replacement) OR (intervertebral disc replacement) OR (screw) OR (rod) OR (cage) OR (adjacent segment disease) OR (adjacent segment degeneration)).

Dose Reduction in Interventional Procedures

- ((computed tomography) OR (CT)) AND ((low-dose) OR (low dose) OR (dose reduction) OR (low-kilovolt) OR (low kilovolt) OR (low-kV) OR (low kV) OR (iterative reconstruction)) AND ((periradicular infiltration) OR (periradicular therapy) OR (periradicular intervention) OR (PRT) OR (epidural injection) OR (epidural steroid injection) OR (ESI) OR (facet joint infiltration) OR (facet joint therapy) OR (facet joint intervention) OR (facet infiltration) OR (facet therapy) OR (facet intervention) OR (FJI) OR (spinal injection) OR (lumbar puncture) OR (LP) OR (intrathecal administration) OR (intrathecal injection) OR (disc biopsy) OR (vertebral biopsy) OR (vertebral body biopsy) OR (spinal biopsy)).

Funding M. Dieckmeyer and N. Sollmann have received funding by the German Society of Musculoskeletal Radiology (Deutsche Gesellschaft für Muskuloskeletale Radiologie, DGMSR). J.S. Kirschke and T. Baum have received funding by the German Research Foundation (Deutsche Forschungsgemeinschaft, DFG; project 432290010). J.S. Kirschke has received funding by European Research Council (ERC) under the European Union Horizon 2020 research and innovation programme (grant agreement No 963904—Bonescreen—ERC-2020-POC-LS).

Funding Open Access funding enabled and organized by Projekt DEAL.

Conflict of interest M. Dieckmeyer, N. Sollmann, K. Kupfer, M.T. Löffler, K.J. Paprottka, J.S. Kirschke and T. Baum declare that they have no competing interests.

References

1. Smith-Bindman R, Kwan ML, Marlow EC, Theis MK, Bolch W, Cheng SY, Bowles EJA, Duncan JR, Greenlee RT, Kushi LH, Pole JD, Rahm AK, Stout NK, Weinmann S, Miglioretti DL. Trends in Use of Medical Imaging in US Health Care Systems and in Ontario, Canada, 2000–2016. *JAMA*. 2019;322:843–56.
2. Smith-Bindman R, Miglioretti DL, Johnson E, Lee C, Feigelson HS, Flynn M, Greenlee RT, Kruger RL, Hornbrook MC, Roblin D, Solberg LI, Vanneman N, Weinmann S, Williams AE. Use of diagnostic imaging studies and associated radiation exposure for patients enrolled in large integrated health care systems, 1996–2010. *JAMA*. 2012;307:2400–9.
3. Brenner DJ, Hall EJ. Computed tomography—an increasing source of radiation exposure. *N Engl J Med*. 2007;357:2277–84.
4. Smith-Bindman R, Lipson J, Marcus R, Kim KP, Mahesh M, Gould R, Berrington de González A, Miglioretti DL. Radiation dose associated with common computed tomography examinations and the associated lifetime attributable risk of cancer. *Arch Intern Med*. 2009;169:2078–86.
5. Richards PJ, George J. Diagnostic CT radiation and cancer induction. *Skelet Radiol*. 2010;39:421–4.
6. Berrington de González A, Mahesh M, Kim KP, Bhargavan M, Lewis R, Mettler F, Land C. Projected cancer risks from computed tomographic scans performed in the United States in 2007. *Arch Intern Med*. 2009;169:2071–7.
7. Bevelacqua JJ. Practical and effective ALARA. *Health Phys*. 2010;98(Suppl 2):S39–S47.
8. Prasad KN, Cole WC, Haase GM. Radiation protection in humans: extending the concept of as low as reasonably achievable (ALARA) from dose to biological damage. *Br J Radiol*. 2004;77:97–9.
9. Demb J, Chu P, Nelson T, Hall D, Seibert A, Lamba R, Boone J, Krishnam M, Cagnon C, Bostani M, Gould R, Miglioretti D, Smith-Bindman R. Optimizing Radiation Doses for Computed Tomography Across Institutions: Dose Auditing and Best Practices. *JAMA Intern Med*. 2017;177:810–7.
10. Smith-Bindman R, Moghadassi M, Wilson N, Nelson TR, Boone JM, Cagnon CH, Gould R, Hall DJ, Krishnam M, Lamba R, McNitt-Gray M, Seibert A, Miglioretti DL. Radiation Doses in Consecutive CT Examinations from Five University of California Medical Centers. *Radiology*. 2015;277:134–41.
11. Roub LW, Drayer BP. Spinal computed tomography: limitations and applications. *AJR Am J Roentgenol*. 1979;133:267–73.
12. Ghodasara N, Yi PH, Clark K, Fishman EK, Farshad M, Fritz J. Postoperative spinal CT: what the radiologist needs to know. *Radiographics*. 2019;39:1840–61.
13. Jo AS, Wilseck Z, Manganaro MS, Ibrahim M. Essentials of spine trauma imaging: radiographs, CT, and MRI. *Semin Ultrasound CT MR*. 2018;39:532–50.
14. Lell MM, Kachelriess M. Recent and upcoming technological developments in computed tomography: high speed, low dose, deep learning, multienergy. *Invest Radiol*. 2020;55:8–19.
15. Willeminck MJ, Noel PB. The evolution of image reconstruction for CT—from filtered back projection to artificial intelligence. *Eur Radiol*. 2019;29:2185–95.
16. Vollmar SV, Kalender WA. Reduction of dose to the female breast in thoracic CT: a comparison of standard-protocol, bismuth-shielded, partial and tube-current-modulated CT examinations. *Eur Radiol*. 2008;18:1674–82.
17. Weis M, Henzler T, Nance JW Jr, Haubenreisser H, Meyer M, Sudarski S, Schoenberg SO, Neff KW, Hagelstein C. Radiation dose comparison between 70kVp and 100kVp with spectral beam shaping for non-contrast-enhanced pediatric chest computed tomography: a prospective randomized controlled study. *Invest Radiol*. 2017;52:155–62.
18. Kalender WA, Wolf H, Suess C. Dose reduction in CT by anatomically adapted tube current modulation. II. Phantom measurements. *Med Phys*. 1999;26:2248–53.
19. Mulkens TH, Bellinck P, Baeyaert M, Ghysen D, Van Dijck X, Mussen E, Venstermans C, Termote JL. Use of an automatic exposure control mechanism for dose optimization in multi-detector row CT examinations: clinical evaluation. *Radiology*. 2005;237:213–23.
20. Solomon JB, Li X, Samei E. Relating noise to image quality indicators in CT examinations with tube current modulation. *AJR Am J Roentgenol*. 2013;200:592–600.
21. Wiedmann U, Neculaes VB, Harrison D, Asma E, Kinahan PE, De Man B. X-ray pulsing methods for reduced-dose computed tomography in PET/CT attenuation correction. In: Whiting BR, Hoeschen C, editors. *Medical imaging 2014: physics of medical imaging*. 2014. p. 90332Z.
22. Koesters T, Knoll F, Sodickson A, Sodickson D, Otazo R. SparseCT: interrupted-beam acquisition and sparse reconstruction for radiation dose reduction. *SPIE*. 2017.

23. Kopp F, Bippus R, Sauter A, Muenzel D, Bergner F, Mei K, Dangelmaier J, Schwaiger BJ, Catalano M, Fingerle AA, Rummeny EJ, Noël PB. Diagnostic value of sparse sampling computed tomography for radiation dose reduction: initial results. *SPIE*. 2018;10573:6
24. Fleischmann D, Boas FE. Computed tomography—old ideas and new technology. *Eur Radiol*. 2011;21:510–7.
25. McCollough CH, Leng S. Use of artificial intelligence in computed tomography dose optimisation. *Ann ICRP*. 2020;49:113–25.
26. Wolterink JM, Leiner T, Viergever MA, Isgum I. Generative adversarial networks for noise reduction in low-dose CT. *IEEE Trans Med Imaging*. 2017;36:2536–45.
27. Chen H, Zhang Y, Kalra MK, Lin F, Chen Y, Liao P, Zhou J, Wang G. Low-dose CT with a residual encoder-decoder convolutional neural network. *IEEE Trans Med Imaging*. 2017;36:2524–35.
28. Chen H, Zhang Y, Zhang W, Liao P, Li K, Zhou J, Wang G. Low-dose CT via convolutional neural network. *Biomed Opt Express*. 2017;8:679–94.
29. Missert AD, Yu L, Leng S, Fletcher JG, McCollough CH. Synthesizing images from multiple kernels using a deep convolutional neural network. *Med Phys*. 2020;47:422–30.
30. Moher D, Liberati A, Tetzlaff J, Altman DG; PRISMA Group. Preferred reporting items for systematic reviews and meta-analyses: the PRISMA Statement. *Open Med*. 2009;3:e123–30.
31. Liberati A, Altman DG, Tetzlaff J, Mulrow C, Gøtzsche PC, Ioannidis JP, Clarke M, Devereaux PJ, Kleijnen J, Moher D. The PRISMA statement for reporting systematic reviews and meta-analyses of studies that evaluate health care interventions: explanation and elaboration. *PLoS Med*. 2009;6:e1000100.
32. Sollmann N, Mei K, Schön S, Riederer I, Kopp FK, Löffler MT, Probst M, Rummeny EJ, Zimmer C, Kirschke JS, Noël PB, Baum T. Systematic evaluation of low-dose MDCT for planning purposes of lumbosacral periradicular infiltrations. *Clin Neuroradiol*. 2020;30:749–59.
33. Mueck FG, Roesch S, Geyer L, Scherr M, Seidenbusch M, Stahl R, Deak Z, Wirth S. Emergency CT head and neck imaging: effects of swimmer's position on dose and image quality. *Eur Radiol*. 2014;24:969–79.
34. Artner J, Lattig F, Reichel H, Cakir B. Effective radiation dose reduction in computed tomography-guided spinal injections: a prospective, comparative study with technical considerations. *Orthop Rev (Pavia)*. 2012;4:e24.
35. Maxfield MW, Schuster KM, McGillicuddy EA, Young CJ, Ghita M, Bokhari SA, Oliva IB, Brink JA, Davis KA. Impact of adaptive statistical iterative reconstruction on radiation dose in evaluation of trauma patients. *J Trauma Acute Care Surg*. 2012;73:1406–11.
36. Geyer LL, Körner M, Hempel R, Deak Z, Mueck FG, Linsenmaier U, Reiser MF, Wirth S. Evaluation of a dedicated MDCT protocol using iterative image reconstruction after cervical spine trauma. *Clin Radiol*. 2013;68:e391–6.
37. Patro SN, Chakraborty S, Sheikh A. The use of adaptive statistical iterative reconstruction (ASiR) technique in evaluation of patients with cervical spine trauma: impact on radiation dose reduction and image quality. *Br J Radiol*. 2016;89:20150082.
38. Yang CH, Wu TH, Chiou YY, Hung SC, Lin CJ, Chen YC, Sheu MH, Guo WY, Chiu CF. Imaging quality and diagnostic reliability of low-dose computed tomography lumbar spine for evaluating patients with spinal disorders. *Spine J*. 2014;14:2682–90.
39. Yang CH, Wu TH, Lin CJ, Chiou YY, Chen YC, Sheu MH, Guo WY, Chiu CF. Knowledge-based iterative model reconstruction technique in computed tomography of lumbar spine lowers radiation dose and improves tissue differentiation for patients with lower back pain. *Eur J Radiol*. 2016;85:1757–64.
40. Iyama Y, Nakaura T, Iyama A, Kidoh M, Katahira K, Oda S, Utsunomiya D, Yamashita Y. Feasibility of Iterative Model Reconstruction for Unenhanced Lumbar CT. *Radiology*. 2017;284:153–60.
41. Shrimpton PC, Jessen KA, Geleijns J, Panzer W, Tosi G. Reference doses in computed tomography. *Radiat Prot Dosimetry*. 1998;80:55–9.
42. McNitt-Gray MF. AAPM/RSNA physics tutorial for residents: topics in CT. Radiation dose in CT. *Radiographics*. 2002;22:1541–53.
43. Bongartz G, Golding SJ, Jurik AG, Leonardi M, van Persijn van Meerten E, Rodríguez R, Schneider K, Calzado A, Geleijns J, Jessen KA, Panzer W, Shrimpton PC, Tosi G. European guidelines for multislice computed tomography. 2004; <http://www.dr.dk/guidelines/ct/quality/index.htm>
44. Committee DICC. AAPM Report No. 096—The measurement, reporting, and management of radiation dose in CT. College Park: Committee DICC; 2008. pp. 20740–3846.
45. Huda W, Ogden KM, Khorasani MR. Converting dose-length product to effective dose at CT. *Radiology*. 2008;248:995–1003.
46. Deak PD, Smal Y, Kalender WA. Multisession CT protocols: sex- and age-specific conversion factors used to determine effective dose from dose-length product. *Radiology*. 2010;257:158–66.
47. Leng S, Christner JA, Carlson SK, Jacobsen M, Vrieze TJ, Atwell TD, McCollough CH. Radiation dose levels for interventional CT procedures. *AJR Am J Roentgenol*. 2011;197:W97–103.
48. Miller TS, Fruauff K, Farinhas J, Pasquale D, Romano C, Schoenfeld AH, Brook A. Lateral decubitus positioning for cervical nerve root block using CT image guidance minimizes effective radiation dose and procedural time. *AJNR Am J Neuroradiol*. 2013;34:23–8.
49. Shrimpton PC, Jansen JT, Harrison JD. Updated estimates of typical effective doses for common CT examinations in the UK following the 2011 national review. *Br J Radiol*. 2016;89:20150346.
50. Greffier J, Pereira FR, Viala P, Macri F, Beregi JP, Larbi A. Interventional spine procedures under CT guidance: how to reduce patient radiation dose without compromising the successful outcome of the procedure? *Phys Med*. 2017;35:88–96.
51. Heggie JC. Patient doses in multi-slice CT and the importance of optimisation. *Australas Phys Eng Sci Med*. 2005;28:86–96.
52. Lee SH, Yun SJ, Jo HH, Kim DH, Song JG, Park YS. Diagnostic accuracy of low-dose versus ultra-low-dose CT for lumbar disc disease and facet joint osteoarthritis in patients with low back pain with MRI correlation. *Skelet Radiol*. 2018;47:491–504.
53. Shepherd TM, Hess CP, Chin CT, Gould R, Dillon WP. Reducing patient radiation dose during CT-guided procedures: demonstration in spinal injections for pain. *AJNR Am J Neuroradiol*. 2011;32:1776–82.
54. Artner J, Cakir B, Weckbach S, Reichel H, Lattig F. Radiation dose reduction in CT-guided periradicular injections in lumbar spine: Feasibility of a new institutional protocol for improved patient safety. *Patient Saf Surg*. 2012;6:19.
55. Artner J, Cakir B, Reichel H, Lattig F. Radiation dose reduction in CT-guided sacroiliac joint injections to levels of pulsed fluoroscopy: a comparative study with technical considerations. *J Pain Res*. 2012;5:265–9.
56. Paik NC. Radiation dose reduction in CT fluoroscopy-guided lumbar interlaminar epidural steroid injection by minimizing preliminary planning imaging. *Eur Radiol*. 2014;24:2109–17.
57. Paik NC. Radiation dose reduction in CT fluoroscopy-guided cervical transforaminal epidural steroid injection by modifying scout and planning steps. *Cardiovasc Intervent Radiol*. 2016;39:591–9.
58. Amrhein TJ, Schauburger JS, Kranz PG, Hoang JK. Reducing patient radiation exposure from CT fluoroscopy-guided lumbar spine pain injections by targeting the planning CT. *AJR Am J Roentgenol*. 2016;206:390–4.
59. Elsholtz FHJ, Kamp JE, Vahldiek JL, Hamm B, Niehues SM. Periradicular infiltration of the cervical spine: how new CT scanner techniques and protocol modifications contribute to the achievement of low-dose interventions. *Rofo*. 2019;191:54–61.
60. Paprottka KJ, Kupfer K, Schultz V, Beer M, Zimmer C, Baum T, Kirschke JS, Sollmann N. Low-dose multi-detector computed to-

- mography for periradicular infiltrations at the cervical and lumbar spine. *Sci Rep.* 2022;12:4324.
61. Ardley ND, Lau KK, Buchan K. Radiation dose reduction using a neck detection algorithm for single spiral brain and cervical spine CT acquisition in the trauma setting. *Emerg Radiol.* 2013;20:493–7.
 62. Lee SH, Yun SJ, Kim DH, Jo HH, Song JG, Park YS. Diagnostic usefulness of low-dose lumbar multi-detector CT with iterative reconstruction in trauma patients: a comparison with standard-dose CT. *Br J Radiol.* 2017;90:20170181.
 63. Weinrich JM, Well L, Regier M, Behzadi C, Sehner S, Adam G, Laqmani A. MDCT in suspected lumbar spine fracture: comparison of standard and reduced dose settings using iterative reconstruction. *Clin Radiol.* 2018;73:675.e9–15.
 64. Lee SH, Yun SJ, Jo HH, Song JG. Diagnosis of lumbar spinal fractures in emergency department: low-dose versus standard-dose CT using model-based iterative reconstruction. *Clin Imaging.* 2018;50:216–22.
 65. Tozakidou M, Yang SR, Kovacs BK, Szucs-Farkas Z, Studler U, Schindera S, Hirschmann A. Dose-optimized computed tomography of the cervical spine in patients with shoulder pull-down: Is image quality comparable with a standard dose protocol in an emergency setting? *Eur J Radiol.* 2019;120:108655.
 66. Sensakovic WF, O'Dell MC, Agha A, Woo R, Varich L. CT Radiation Dose Reduction in Robot-assisted Pediatric Spinal Surgery. *Spine (Phila Pa 1976).* 2017;42:E417–24.
 67. Mulkens TH, Marchal P, Daineffe S, Salgado R, Bellinck P, te Rijdt B, Kegelaers B, Termote JL. Comparison of low-dose with standard-dose multidetector CT in cervical spine trauma. *AJNR Am J Neuroradiol.* 2007;28:1444–50.
 68. Elsholtz FHJ, Schaafs LA, Kohlitz T, Hamm B, Niehues SM. Periradicular infiltration of the lumbar spine: testing the robustness of an interventional ultra-low-dose protocol at different body mass index levels. *Acta Radiol.* 2017;58:1364–70.
 69. Rosiak G, Lusakowska A, Milczarek K, Konecki D, Fraczek A, Rowinski O, Kostera-Pruszczyk A. Ultra-low radiation dose protocol for CT-guided intrathecal nusinersen injections for patients with spinal muscular atrophy and severe scoliosis. *Neuroradiology.* 2021;63:539–45.
 70. Abul-Kasim K, Overgaard A, Maly P, Ohlin A, Gunnarsson M, Sundgren PC. Low-dose helical computed tomography (CT) in the perioperative workup of adolescent idiopathic scoliosis. *Eur Radiol.* 2009;19:610–8.
 71. Shpilberg KA, Delman BN, Tanenbaum LN, Esses SJ, Subramaniam R, Doshi AH. Radiation dose reduction in CT-guided spine biopsies does not reduce diagnostic yield. *AJNR Am J Neuroradiol.* 2014;35:2243–7.
 72. Cordts I, Deschauer M, Lingor P, Burian E, Baum T, Zimmer C, Maegerlein C, Sollmann N. Radiation dose reduction for CT-guided intrathecal nusinersen administration in adult patients with spinal muscular atrophy. *Sci Rep.* 2020;10:3406.
 73. Anitha D, Mei K, Dieckmeyer M, Kopp FK, Sollmann N, Zimmer C, Kirschke JS, Noel PB, Baum T, Subburaj K. MDCT-based finite element analysis of vertebral fracture risk: what dose is needed? *Clin Neuroradiol.* 2019;29:645–51.
 74. Sollmann N, Mei K, Riederer I, Schön S, Kirschke JS, Meyer B, Zimmer C, Baum T, Noël PB. Low-Dose MDCT of Patients With Spinal Instrumentation Using Sparse Sampling: Impact on Metal Artifacts. *AJR Am J Roentgenol.* 2021;216:1308–17.
 75. Mei K, Kopp FK, Bippus R, Köhler T, Schwaiger BJ, Gersing AS, Fehringer A, Sauter A, Münzel D, Pfeiffer F, Rummeny EJ, Kirschke JS, Noël PB, Baum T. Is multidetector CT-based bone mineral density and quantitative bone microstructure assessment at the spine still feasible using ultra-low tube current and sparse sampling? *Eur Radiol.* 2017;27:5261–71.
 76. Sollmann N, Mei K, Hedderich DM, Maegerlein C, Kopp FK, Löffler MT, Zimmer C, Rummeny EJ, Kirschke JS, Baum T, Noël PB. Multi-detector CT imaging: impact of virtual tube current reduction and sparse sampling on detection of vertebral fractures. *Eur Radiol.* 2019;29:3606–16.
 77. Sollmann N, Mei K, Riederer I, Probst M, Löffler MT, Kirschke JS, Noël PB, Baum T. Low-dose MDCT: evaluation of the impact of systematic tube current reduction and sparse sampling on the detection of degenerative spine diseases. *Eur Radiol.* 2021;31:2590–600.
 78. Månsson LG. Methods for the evaluation of image quality: a review. *Radiat Prot Dosimetry.* 2000;90:89–99.
 79. Cohen J. A coefficient of agreement for nominal scales. *Educ Psychol Meas.* 1960;20:37–46.
 80. Landis JR, Koch GG. The measurement of observer agreement for categorical data. *Biometrics.* 1977;33:159–74.
 81. Bohy P, de Maertelaer V, Roquigny A, Keyzer C, Tack D, Gevenois PA. Multidetector CT in patients suspected of having lumbar disk herniation: comparison of standard-dose and simulated low-dose techniques. *Radiology.* 2007;244:524–31.
 82. Schauburger JS, Kranz PG, Choudhury KR, Eastwood JD, Gray L, Hoang JK. CT-guided lumbar nerve root injections: are we using the correct radiation dose settings? *AJNR Am J Neuroradiol.* 2012;33:1855–9.
 83. Elsholtz FHJ, Schaafs LA, Erxleben C, Hamm B, Niehues SM. Ultra-low-dose periradicular infiltration of the lumbar spine: spot scanning and its potential for further dose reduction by replacing helical planning CT. *Radiol Med.* 2017;122:705–12.
 84. Mercuri E, Finkel RS, Muntoni F, Wirth B, Montes J, Main M, Mazzone ES, Vitale M, Snyder B, Quijano-Roy S, Bertini E, Davis RH, Meyer OH, Simonds AK, Schroth MK, Graham RJ, Kirschner J, Iannaccone ST, Crawford TO, Woods S, Qian Y, Sejersen T; SMA Care Group. Diagnosis and management of spinal muscular atrophy: Part 1: Recommendations for diagnosis, rehabilitation, orthopedic and nutritional care. *Neuromuscul Disord.* 2018;28:103–15.
 85. Kanal KM, Butler PF, Sengupta D, Bhargavan-Chatfield M, Coombs LP, Morin RL. U.S. Diagnostic reference levels and achievable doses for 10 adult CT examinations. *Radiology.* 2017;284:120–33.
 86. Bos D, Yu S, Luong J, Chu P, Wang Y, Einstein AJ, Starkey J, Delman BN, Duong PT, Das M, Schindera S, Goode AR, MacLeod F, Wetter A, Neill R, Lee RK, Roehm J, Seibert JA, Cervantes LF, Kasraie N, Pike P, Pahwa A, Jeukens CRLPN, Smith-Bindman R. Diagnostic reference levels and median doses for common clinical indications of CT: findings from an international registry. *Eur Radiol.* 2022;32:1971–82.
 87. Sauter AP, Kopp FK, Bippus R, Dangelmaier J, Deniffel D, Fingerle AA, Meurer F, Pfeiffer D, Proksa R, Rummeny EJ, Noël PB. Sparse sampling computed tomography (SpSCT) for detection of pulmonary embolism: a feasibility study. *Eur Radiol.* 2019;29:5950–60.
 88. Long Z, DeLone DR, Kotsenas AL, Lehman VT, Nagelschneider AA, Michalak GJ, Fletcher JG, McCollough CH, Yu L. Clinical Assessment of Metal Artifact Reduction Methods in Dual-Energy CT Examinations of Instrumented Spines. *AJR Am J Roentgenol.* 2019;212:395–401.
 89. Willeminck MJ, Persson M, Pourmorteza A, Pelc NJ, Fleischmann D. Photon-counting CT: technical principles and clinical prospects. *Radiology.* 2018;289:293–312.
 90. Flohr T, Petersilka M, Henning A, Ulzheimer S, Ferda J, Schmidt B. Photon-counting CT review. *Phys Med.* 2020;79:126–36.